JOURNAL OF AEROSPACE SOCIETY MALAYSIA

ARTICLE

AERODYNAMIC ANALYSIS OF UiTM'S ENERGY GLIDER WITH FITTED WINGLETS USING CFD SIMULATION

Zurriati Mohd Ali [1,*], Jasmine Demi anak Danny Jabing [1], Hasman Selle [1] and Nurul Balqis Hosni [1]

1. School of Mechanical Engineering, College of Engineering, Universiti Teknologi MARA (UiTM), 40450 Shah Alam, Selangor, Malaysia.

Correspondence: * zurriatimohdali@uitm.edu.my

Abstract: Gliders are aircraft with fixed wings that do not depend on an engine to fly. Depending on the design and size of the lifting surface, gliders can fly for long distances. Like other types of aircraft, wings of the glider must be designed in such a way as to provide lift to maintain flight level. The long, slender wings and lightweight design provide gliders with maximum lift-to-drag ratio. The purpose of this study is to determine the aerodynamic characteristics (i.e. lift, drag and moment) of UiTM's energy glider that has been incorporated with winglets, which are vertical wingtip extensions that can increase the aircraft's fuel efficiency and cruising range. In this study, the KFm-5a is used as the airfoil profile for the glider's wing. The glider is modelled using CATIA and the resultant model is then exported to Fluent Ansys, which is a computational fluid dynamic (CFD) analysis software. For the CFD analysis, the flow around the glider's model is simulated at Reynolds number of 4.7 x 10^5 and Mach number 0.1 (~35 m/s). The turbulence model used in this study is Spalart-Allmaras due to its efficiency in reducing the complexity of the problem and also the overall simulation time. The aircraft is pitched at a range of angles of attack from -2° until it reaches the stall angle with an interval of 2°. On the whole, the results show that the glider with the winglet has higher maximum lift-to-drag ratio of 13.7 at angle of attack of 4° as compared to the original glider without the winglet that has a maximum lift-to-drag ratio of only 12.4 at the same angle of attack. Nevertheless, the differences of lift and drag forces between these two glider configurations can be taken to be relatively small.

Keywords: glider; CFD; aircraft; aerodynamics; Fluent Ansys

1. Introduction

Gliders have a long range of flight that depends on the design and size of the lifting surface. Most modern gliders have a glide ratio that is greater than 60:1. In comparison to Boeing 747 aircraft, which is a conventional aircraft with glide ratio of 15:1, the gliders can glide for 96.6 km at a height of 1.6 km above sea level [1]. Some gliders have an altitude gliding engine that can be turned off once the necessary lift has been produced. Since the gliders can glide without relying on the engine, this enables it to have minimal environmental impact as the air pollution from engine combustion is reduced when flying the gliders. There are numerous different varieties of gliders, each with a unique wing design, aerodynamic efficiency, pilot position, controls, and intended usage. Typically, basic lightweight materials like wood, plastic and foam are used to make gliders. From the aerodynamics point of view, a glider can be referred to as 'heavier-than-air' aircraft that glides through air due to the dynamic reaction of air against its lifting surface [2]-[3]. Principle aerodynamic forces like weight (W), lift (L), thrust (T) and drag (D) are what enable gliders to fly. These principles will determine the glider's speed and direction of motion – upward

and downward. Generally, the main objectives of the energy glider design are to create an aircraft that can fly for as long as possible, for recreational uses (air sports and toys) and for further research.

The Kline-Fogleman airfoil is also known as the KFm airfoil, which is a simple airfoil in which the steps run in the direction of the chord length. The steps can be single or multiple. This KFm airfoil was designed by Richard Kline and Floyd Fogleman when he was experimenting with a high-strength paper airplane that would glide well, and after much experimentation, he was able to achieve this goal. Richard and Floyd found that this stepped airfoil concept was capable of resisting stall, whereupon they decided to apply for patent on this stepped airfoil [4]. In addition, such airfoil with the stepped upper surface could offer higher lift coefficient, higher lift-to-drag ratio and high stall angle [5]. This particular airfoil has a step in 50% chord with 50% depth [6]. Moreover, flight performance is greatly affected by drag created by vortices at the wing tips. Winglets are extensions of the wingtips and are used to minimize vortex formation, thereby improving fuel efficiency [7]. They are typically used on heavier cargo aircraft due to higher operating costs and higher fuel consumption on long-haul missions. The improvement in aircraft performance provided by winglets results largely from their ability to reduce induced drag, which is offset by their additional wetted area that increases profile drag. Profile drag is the drag created by the shape of the airfoil or wing section. Induced drag is the drag resulting from the generation of lift by a bounded wing [8]-[9]. In this study, the simplest and most commonly used winglet is used, which is the blended winglet. The blended winglet consists of an upwardly offset blade extension. Compared to many other types, the mixed wing is characterized by a smooth chord transition instead of an angular transition from wing to winglet. Even with simple, non-optimized design implementations, significant lift and drag improvements of almost 9% can be observed. The design has been initially researched by Boeing in the mid-1980s and developed by Aviation Partners Inc. in the early 1990s [10].

UiTM's energy glider has been the subject of a prior research. Its design, construction and flight testing all took place at UiTM Shah Alam. Since the original aircraft was developed for a Radio Control Aircraft, there has been no study to compare the obtained data (i.e. flight testing data) with analytical, numerical and experimental methods. Based on this notion, these are carried out in this study to obtain proper aerodynamic data for this energy glider and add aerodynamic analysis to the current design. The result is then used to improve the design of the energy glider in terms of aerodynamic characteristics. Figure 1 presents the original and downscale of UiTM's energy glider and its specifications. The glider is scaled down to ¼ from its original size.

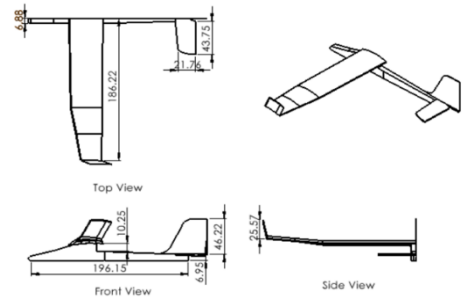

FULL SCALE SIZE	
Wing Span	1490 mm
Wing Area	111000 mm^2
Root Chord	166 mm
Tip Chord	103 mm
Fuselage Length	785 mm

1:4 SCALE DOWN SIZE	
Wing Span	372.5 mm
Wing Area	27750 mm^2
Root Chord	41.5 mm
Tip Chord	25.75 mm
Fuselage Length	196.25 mm

Figure 1: UiTM's Energy Glider and its specifications

The goals of this research are to determine aerodynamic forces such as lift coefficient (C_L), drag coefficient (C_D) and lift-to-drag ratio (L/D) through CFD simulation. The C_L and C_D can be calculated by Equation 1 and Equation 2. In these equations, L is the lift force, D is the drag force, ρ is the density of air, V is the subjected velocity and S is the wing area.

$$C_L = \frac{L}{0.5\rho V^2 S} \tag{1}$$

$$C_D = \frac{D}{0.5\rho V^2 S} \tag{2}$$

In this study, the freestream velocity is fixed at 35 m/s where the corresponding Reynolds number is 4.7 x 10^5 as calculated using Equation 3, where L represents the length of the aircraft and μ is a fluid dynamics viscosity. Moreover, the corresponding Mach number is 0.1 as calculated by using Equation 4, where γ is a specific heat ratio, R is a gas constant and T is a temperature. This indicates that the flow is subsonic.

$$Re = \frac{\rho v L}{\mu} \tag{3}$$

$$M = \frac{V}{\sqrt{\gamma R T}} \tag{4}$$

The flow around the glider is simulated, observed and analysed. The CFD analysis of energy glider performance on ANSYS Fluent is done until the stall angle α_{stall} is achieved. The scaled-down model is used to ease the simulation process. The UITM's energy glider design is for experimental purposes only.

It is shown that the market size of gliders is increasing in demand, both for commercial and military applications. The understanding of gliders' performance has been used to study the aerodynamics and flight control fundamentals. The ever-expanding range of gliders' applications such as in the military for training purposes indicates that the study of design and aerodynamics of energy gliders is vital to produce a better performance and reliable glider. Information gathered from this study can be used to further expand gliders in space exploration as gliders emit little to no pollution that can be harmful to the space environment.

2. Methodology

Figure 2 shows the flowchart of the methodology in this study. In short, this study starts with the measuring of the dimensions of the glider. The measurement data is recorded before the glider is drawn in computer-aided design (CAD) software, CATIA. The scaled-down half model of the glider is created, which allows for detailed visualization of the glider's design including its shape, dimensions and overall geometry. The CATIA file is then converted into .stp file format, which is a neutral file format for CAD data. This file is imported into Ansys Fluent Geometry. By importing the geometry into Ansys Fluent, it becomes possible to perform fluid flow analysis on the glider. A mesh is generated around the glider and its enclosure before going to the set-up section. The mesh size and density are determined based on desired level of accuracy and computational resources available. Additionally, boundary conditions are defined, specifying fluid flow properties and environmental conditions that the glider will experience during the operation. After the meshing process is done, the initial condition of this simulation needed to be set up including solver type, turbulence model, references value and also number of iteration. The

simulation results provide some insights into the glider's aerodynamic performance including lift, drag and other relevant flow characteristics.

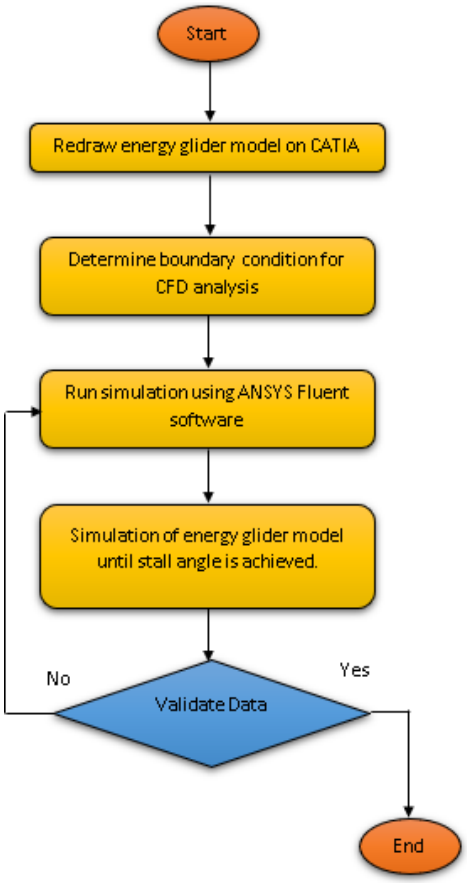

Figure 2: Flowchart of methodology for this study

2.1. Pre-processing

There is no detailed drawing for this aircraft. Therefore, the physical model is measured and drawn manually on CATIA by considering every detail and angle of the existing energy glider. Detailed drawing is required to obtain the most accurate model representation of the energy glider as shown in Figure 3. Compared to the original model, a winglet is added to improve the drag of the glider. The chosen type of winglet in this study is a blended winglet with an angle concerning the main wing of 56°. This blended type is chosen due to its simplest design.

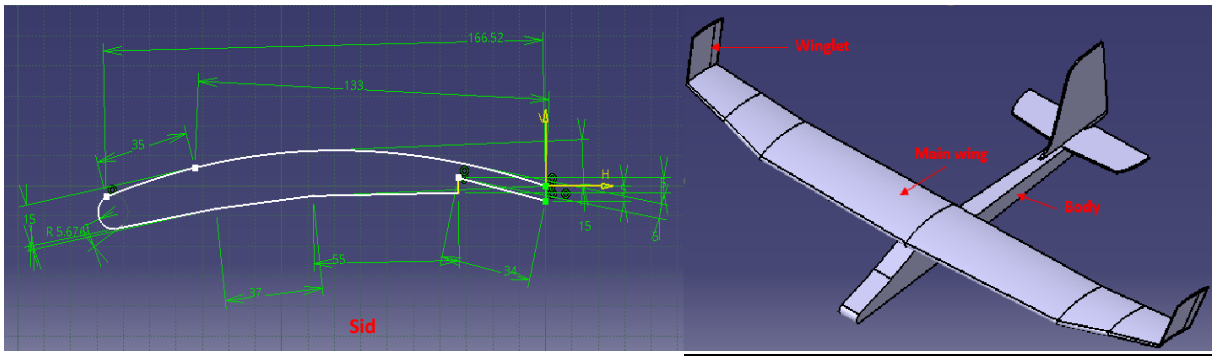

Figure 3: Energy glider fitted with winglets in CAD (in mm)

The glider drawing is then converted into STP file (.stp) to enable the drawing to be imported into Ansys Fluent software for simulation purposes. The drawing has been scaled down by 1-to-4 ratio from the original size to ease the meshing process and to save time for the simulation analysis. Figure 4 shows the drafting of the half-model scaled-down glider from the front view, top view and side view.

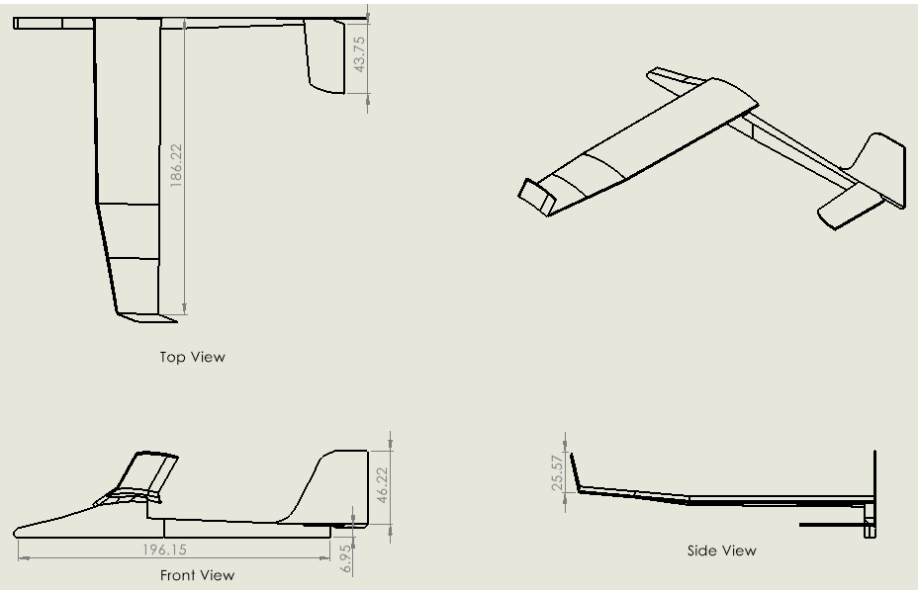

Figure 4: Isometric view of the glider

The early step in Ansys Fluent software is to import the drawing file to the geometry setup. In this section, the body and wing of the energy glider need to combine into one subjected body by Boolean Operation. Figure 5 shows the glider is pitched at angles of attack, α of 0° and 13°. It should be noted that the pitching point is based on the mean aerodynamics center (MAC) of the fuselage.

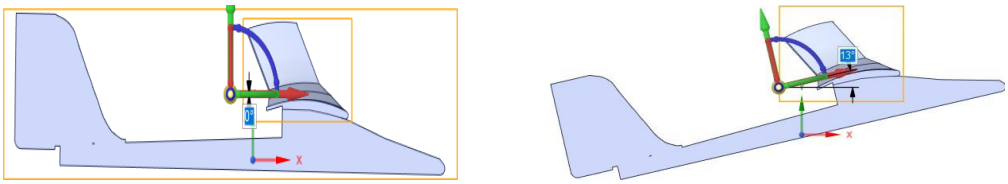

(a) α = 0° (b) α = 13°

Figure 5: Pitching angles

2.2. Meshing

Meshing is the process of dividing the computational domain such as the enclosure created in the geometry, into very small sub-volumes. The process of meshing is extremely critical and great care must be taken to create a mesh to capture the correct flow behavior. The size of the computational domain used in this study is L x W x H = 2.20 m x 1.19 m x 2.05 m, which is shown in Figure 6. This size will affect the total element of mesh and the result of simulation such as the airflow. Boundary condition, addresses how fluid enters and exits the simulation model. This process also includes the changes that have taken place between the model and its environment. In other words, one can also view that the boundary condition connects the model with its environment. The element size chosen for the glider has to be as small as possible to increase the accuracy of the result but this will also subsequently increase the time taken to complete the simulation. A grid independence study has been carried out to minimize the effect of grid size on the computing outcomes. It will generate a series of coarse, medium and fine

meshes to show how the solution varies between different mesh sizes. A grid independence analysis is undertaken and it is observed that the result is converged at the number of elements of about 1,950,000 as shown in Figure 7. This is taken as the reference for the meshing process.

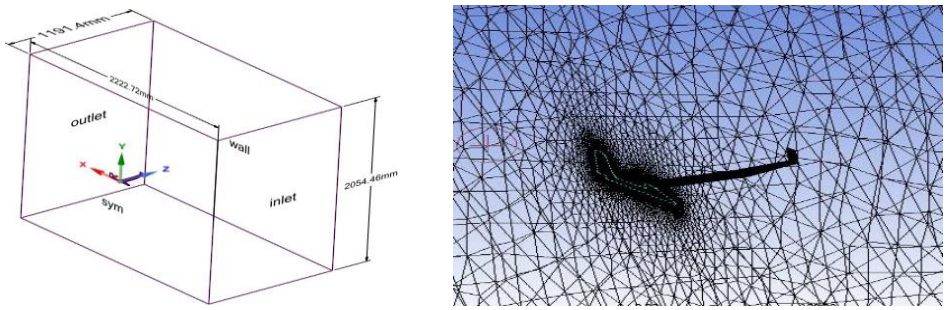

Figure 6: Flow domain and mesh on the glider's body

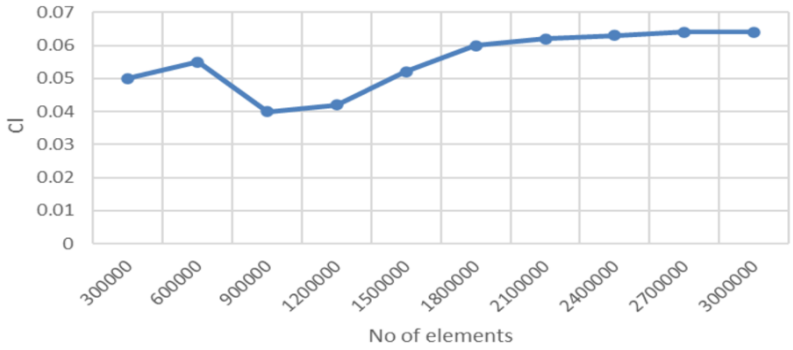

Figure 7: Results of the grid independence study

2.3. Processing

Important parameters such as solver, turbulence model, boundary conditions, reference values and number of iterations have been properly decided to simulate the realistic conditions. The setup is shown in Table 1. The Spalart-Allmaras modeling is used as the turbulence model because it is a simple model for solving a transport equation for turbulent viscosity (kinematic vortices). This model can calculate a local shear layer thickness for the length scale with one equation. The Spalart-Allmaras model has been developed specifically for wall-bounded flows and boundary layers with unfavorable pressure gradients in aerospace applications [11]. Figure 8 shows the residual graph where it shows all the lines which are continuity, x-velocity, y-velocity, z-velocity and nut converge at 198 iterations and undergo 25 minutes of completion time.

Table 1: Setup and solution

Parameter	Value
Solver	Type: Pressure-based; Time: Steady; Velocity formulation: Absolute
Turbulence model	Spalart-Allmaras
Boundary condition	Inlet velocity: 35 m/s; Inlet pressure: 101,325 Pa
Reference Value	Area: 0.008421 m^2; Density: 1.225 kg/m^3; Pressure: 101,325 Pa; Temperature: 297 K; Velocity: 35 m/s
Number of Iteration	200 - 400

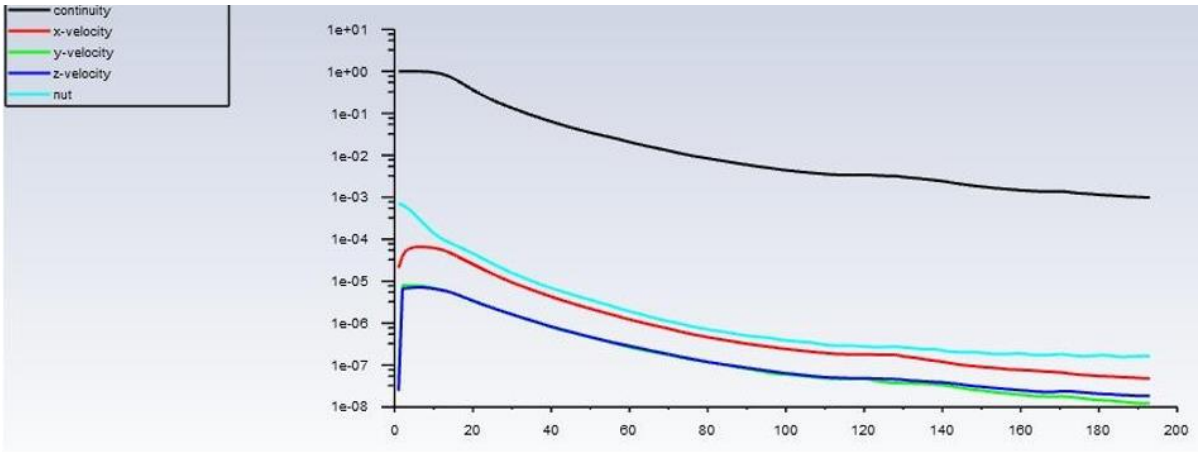

Figure 8: Example residual graph for 200 iterations

2.4. Post-processing

Visualization of the static pressure and the air velocity can be obtained from the simulation results as shown in Figure 9. Pressure contour is used to determine the magnitude of pressure at certain areas of the glider such as its nose as well as the leading and trailing edge of its wing. In addition, a velocity vector is used to represent speed and direction of the airflow in a domain or on a surface. Furthermore, the streamline in Figure 9 also shows the trend of the airflow in a domain or on a surface.

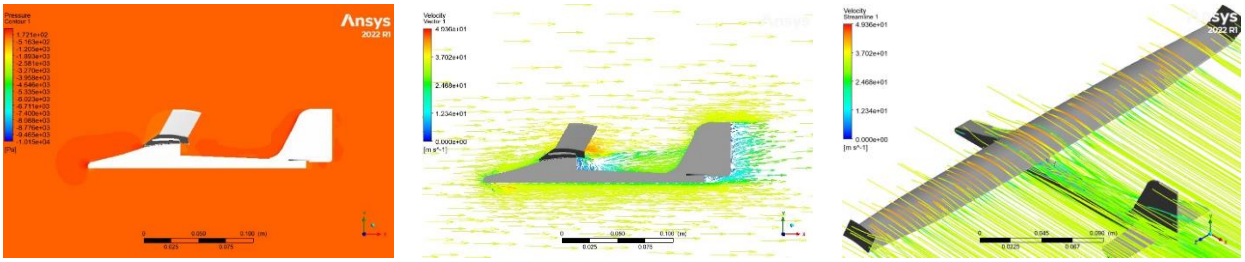

(a) Pressure contour (b) Velocity vector (c) Streamline

Figure 9: Example simulation output results at $\alpha = 0^{o}$

3. Results and Discussion

It is important to compare the aerodynamic performance of the original design with the modified design of the energy glider that is fitted with winglets in terms of C_L, C_D and L/D. It should be noted that the CFD simulation results for the original design of the UiTM's energy glider have been compared to the published data in Ref. [12] for validation process. Data validation can aid in detecting mistakes, as well as improving the accuracy of findings. Overall, the comparison shows that the CFD simulation results in this study match well and consistent with the findings in Ref. [12]. Therefore, the simulation settings used in this study can be taken as adequate to obtain results with a good accuracy.

3.1. Aerodynamics data

Figure 10, Figure 11 and Figure 12 show the relationship of C_L, C_D and L/D against angle of attack, α for the existing energy glider and also the modified energy glider fitted with winglets. In Figure 10, the plot shows the increment of C_L for both gliders (i.e. with and without winglet) when α is increased from 0° until 12°. However, it is observed that the lift force starts to decrease when α is about 14° and

this is called a stall angle, α_{stall}. For the existing glider, its α_{stall} is found to be 14° with a maximum C_L of 1.164 whereas for the modified glider with the winglet, its stall angle is the same but it has slightly higher maximum C_L of 1.173. The lift differences are small, which is just about 0.8%, and rather negligible. In Figure 11, it can be considered that the C_D of both gliders (i.e. with and without winglet) increases in a parabolic manner as α increases. At the stall angle for the existing glider, its C_D is found to be 0.178. On the other hand, for the modified glider with winglets, its C_D is 0.177 at the stall angle. The percentage difference is 7.15% and considerably small. A lower drag coefficient means that the shape of the airfoil with a winglet allows it to move easily through the air with minimum resistance. A lower drag coefficient can improve speed, range and fuel consumption. Since the drag force increases as α increases, it is vital to select the appropriate α at different phases of flight to ensure optimization of the glider's design. In Figure 12, it can be seen that L/D of the modified glider with winglet is higher when compared to that for the original glider design without the winglet. The maximum L/D for the glider without winglet is about 13. 4 while that for the modified glider with winglet is 13.7, which both occurs at α of 4°. This means that the energy glider with a winglet generates a higher maximum L/D. In general, a higher L/D allows the modified energy glider with winglets to fly farther with the same amount of fuel as the original UiTM's energy glider design.

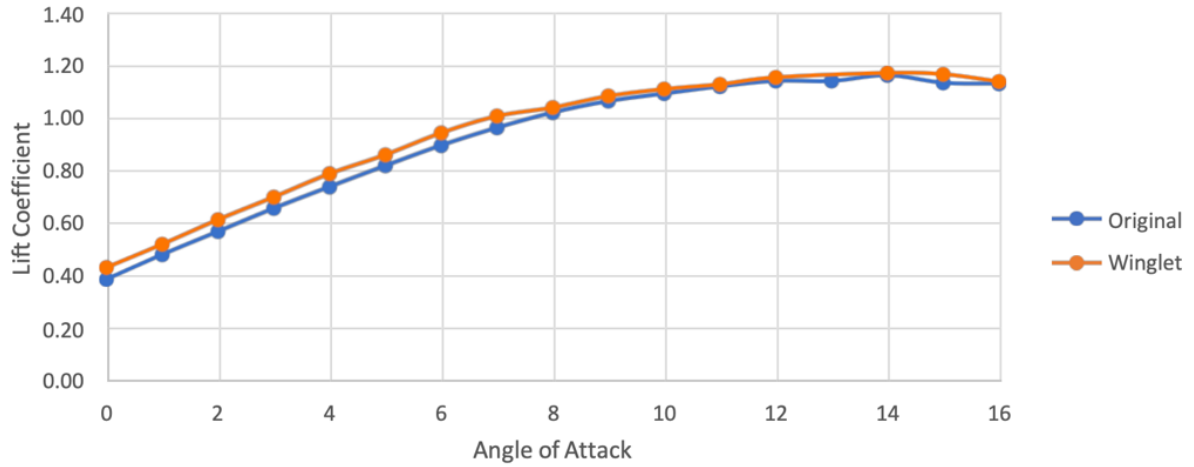

Figure 10: Lift coefficient versus angle of attack

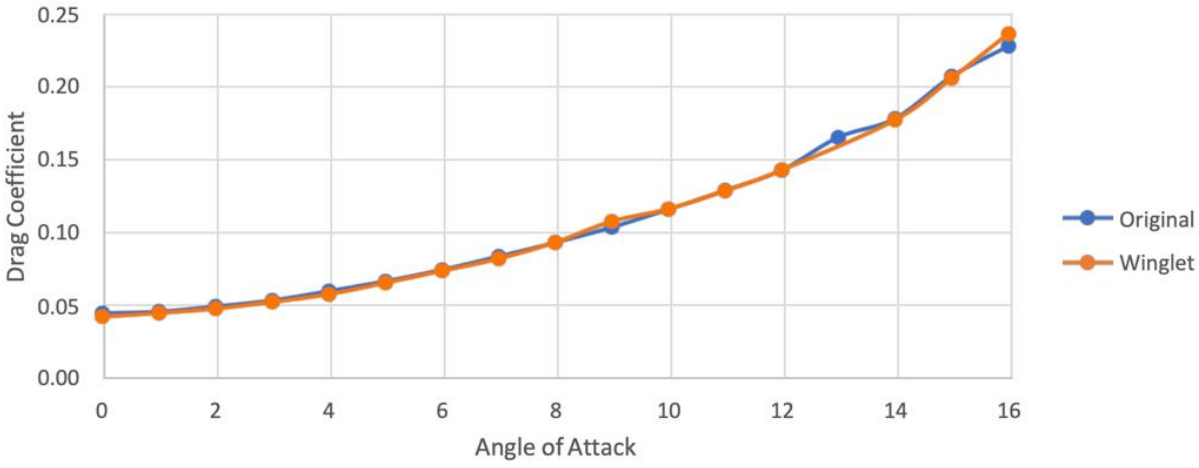

Figure 11: Drag coefficient versus angle of attack

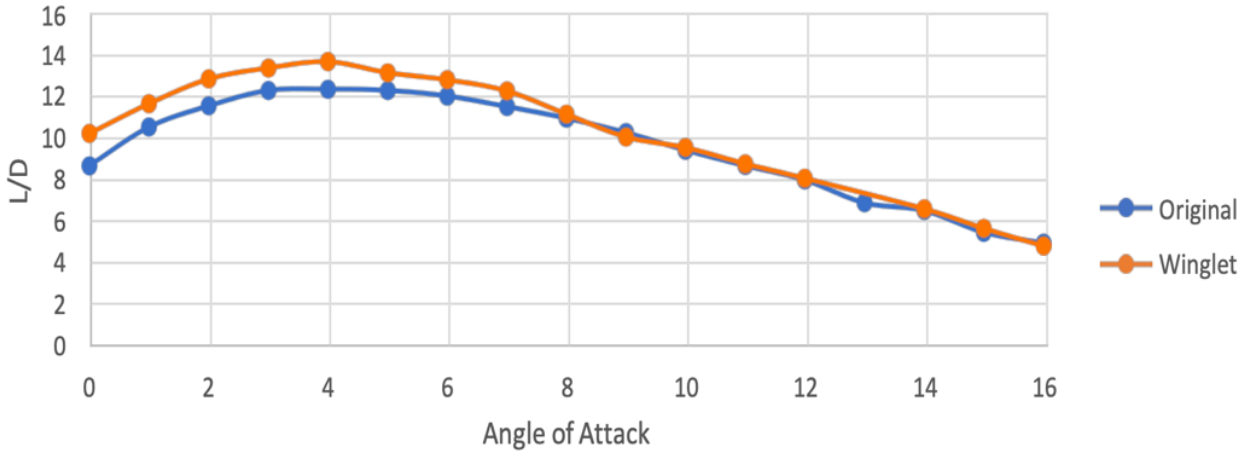

Figure 12: L/D versus angle of attack

3.2. Flow visualization

Figure 13 to Figure 15 are visualizing the flow around the modified glider's body at angles of attack of 0° and 14°. Figure 13 shows that the glider experiences an equal distribution of pressure both at the body and wing at angle of attack of 0°, which is approximately 623.6 Pa. In the same Figure 13 for angle of attack of 14°, the glider encounters a high pressure at the leading edge of the wing and the nose of the glider, which is about 700.9 Pa. Around the glider's body, it experiences pressure of about 79.65 Pa that is quite a small amount as compared to the nose and leading edge. Moreover, Figure 14 shows that the magnitude of the velocity on the glider at angle of attack of 0° is about 49.36 m/s. On the rear of the glider, the velocity is a bit slower, which is about 24.68 m/s. This may be due to the drag force on the body and tail of the glider. At the stall angle of 14°, the velocity magnitude is higher, which is about 64.39 m/s, as compared to when the glider is at angle of attack of 0°. At the trailing edge of the glider for this angle of attack of 14°, the velocity is about 32.19 m/s, which is about 50% of the velocity at the leading edge of the wing. The airflow on the glider at angle of attack of 0° is essentially smooth, or can be described as a laminar flow where there is no reversible flow occurring along the wing of the glider, as shown in Figure 15. In contrast, at stall angle of 14°, there is a separation of the airflow at the trailing edge of the wing. The turbulence flow can be seen in the blended area between the winglet and the main wing. As shown in Figure 15 for angle of attack of 14°, the flow at the winglet is smooth. This shows that the winglet successfully prevents the turbulence flow from occurring at the wingtip and this automatically reduces drag force at the wingtip of the glider.

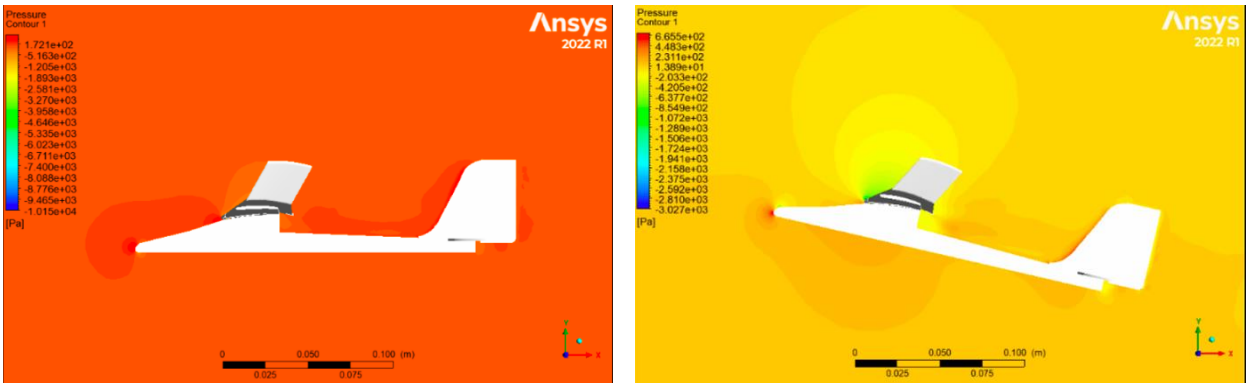

(a) $\alpha = 0°$ (b) $\alpha = 14°$

Figure 13: Pressure contour results from CFD simulation analysis

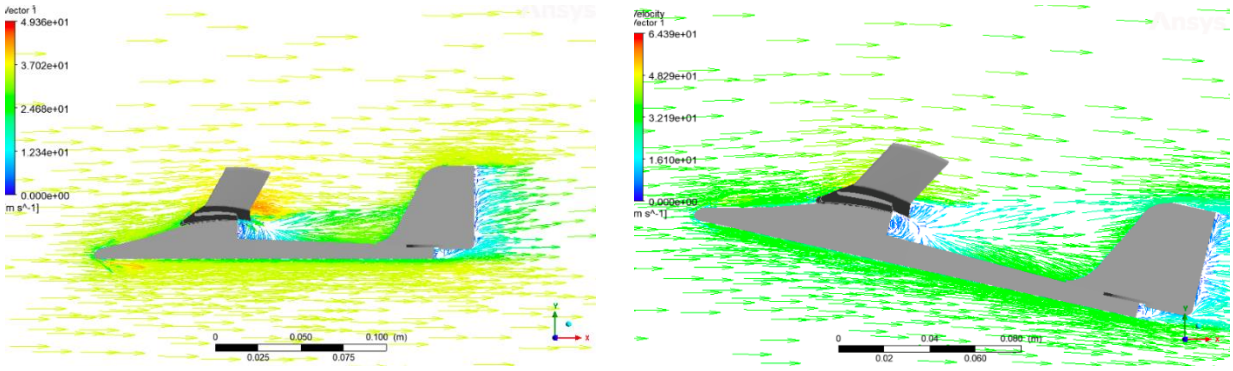

(a) $\alpha = 0°$ b) $\alpha = 14°$

Figure 14: Velocity vector results from CFD simulation analysis

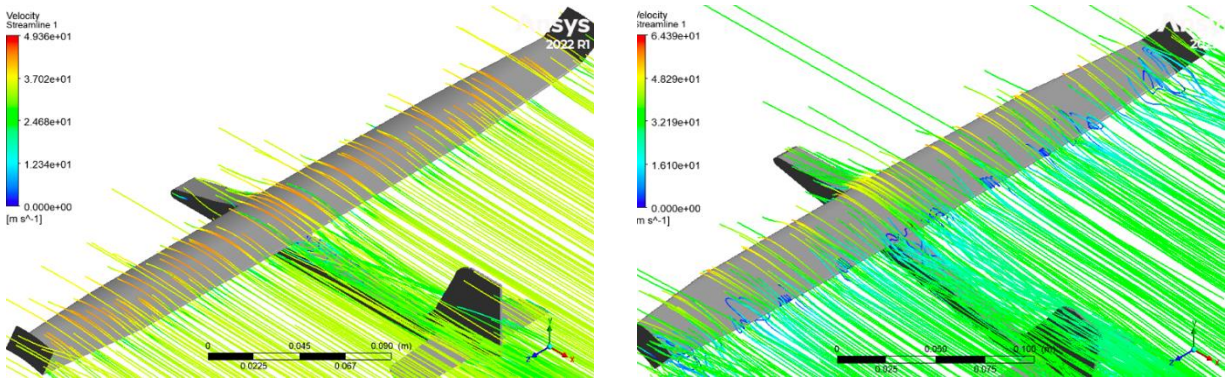

(a) $\alpha = 0°$ (b) $\alpha = 14°$

Figure 15: Velocity streamline results from CFD simulation analysis

4. Conclusion

In this study, the aerodynamic performance characteristics such as C_L, C_D and L/D of the existing energy glider and the modified energy glider with winglets have been successfully determined through CFD simulation in ANSYS Fluent. The obtained CFD results enable the study of the flow around the glider, as well as creating an improved design. There may be limitations faced due to the performance of the model. Overall, the results obtained from this research are proven to be successful and beneficial. Based on the results obtained, the modified UiTM's energy glider design with winglets has been shown to have better aerodynamic performance than existing design, especially in having a higher L/D. Further study can be further conducted in future to improve the glider design.

Acknowledgement

The authors like to express their gratitude to College of Engineering, Universiti Teknologi MARA, Malaysia for providing the facilities and support throughout the completion of this research.

References

[1] S. Martin. (2015). How Gliders Fly and How They're Different Than Powered Aircraft. Retrieved from www.boldmethod.com/blog/article/2015/02/your-guide-to-glider

[2] M. K. A. Muhamad and B. Basuno, 'A Long Endurance of Single Seater Glider Aircraft Design', Journal of Aviation and Aerospace Technology, vol. 1, no. 1, 2019.

[3] Federal Aviation Administration, Glider Flying Handbook, Skyhorse Publishing Inc., 2007.

[4] S. Shriwas, P. Singh, S. Shah and K. P. Kaurase, 'Introduction to Step Wing & Kline Fogleman Airfoil', International Journal for Scientific Research & Development, vol. 3, no. 2, pp. 503-506, 2015.

[5] A. Kabir, Y. M. Akib, A. Hafiz and M. Islam, 'Comparison between Two Kline–Fogleman Modified (KFm) based Stepped Airfoils for Better Aerodynamic Performance', International Conference on Innovation in Engineering and Technology (ICIET), Dhaka, Bangladesh, 23-24 December 2019.

[6] A. Kabir, M. Islam, N. Jahan, Y. M. Akib and M. I. J. Mili, 'Numerical Simulation and Comparative Study of Aerodynamic Performance of Kline Fogleman Modified Backward Stepped Airfoils and the NACA 4415 Airfoil', Bangladesh Maritime Journal, vol. 5, no. 1, pp. 97-110, 2021.

[7] G. Panagi, 'Investigation of Winglet Shapes on Aerodynamic Efficiency View Project', Bachelor Thesis, University of the West of England, 2019.

[8] J. A. D. Ackroyd, 'Cayley's 1804 Glider', Journal of Aeronautical History, vol. 2019, pp. 98-107, 2019.

[9] M. D. Maughmer, 'The Design of Winglets for Low-Speed Aircraft', Technical Soaring, vol. 30, no. 3, pp. 61-73, 2006.

[10] H. Gongzhang and E. Axtelius, 'Aircraft Winglet Design', Project Report, KTH Royal Institute of Technology, 2020.

[11] ANSYS FLUENT 12.0 Theory Guide. Retrieved from www.afs.enea.it/project/neptunius/docs/fluent/html/th/main_pre.htm

[12] S. Hasman, 'Aerodynamics Performance of UiTM's Energy Glider with Winglet using CFD Simulations', Bachelor Thesis, Universiti Teknologi MARA, 2023.